Fast thermistor string observations at the slope of Great Meteor Seamount

H. van Haren, R. Groenewegen, M. Laan, B. Koster

Ocean Science Discussions, 1, 37–64, 2004
www.ocean-science.net/osd/1/37/
SRef-ID: 1812-0822/osd/2004-1-37
European Geosciences Union

Ocean Science Discussions

Fast thermistor string observations at the slope of Great Meteor Seamount

H. van Haren, R. Groenewegen, M. Laan, and B. Koster

Royal Netherlands Institute for Sea Research (NIOZ), P.O. Box 59, 1790 AB Den Burg, The Netherlands

Received: 15 November 2004 – Accepted: 14 December 2004 – Published: 22 December 2004

Correspondence to: H. van Haren (hansvh@nioz.nl)

Abstract

A very fast thermistor string has been built to accommodate the scientific need to accurately monitor fast and vigorous internal wave and overturning processes above sloping bottoms in the ocean. The thermistors and their custom designed electronics can register temperature at an estimated precision of about 1 mK with a response time faster than 0.25 s down to depths of 6000 m. The present string holds 128 synoptically measuring sensors at 0.5 m intervals, which are all read-out within 0.5 s. When sampling at 1 Hz, the batteries and the memory capacity of the recorder allow for deployments of up to 2 weeks. Detailed examples of the first field observations are presented, which show overturning and very high-frequency (Doppler-shifted) internal waves besides occasionally large turbulent bores moving up the sloping side of Great Meteor Seamount, Canary Basin, North-Atlantic Ocean.

1. Introduction

After successful deployments of the first NIOZ thermistor string (NIOZ1: 32 sensors at 1 m intervals, sampled once per 20 s, precision better than 40 μK; van Haren et al., 2001) plans were made to modify the concept, so that it would be better adapted to different environments. Specifically, we wanted to monitor, over periods of a few weeks, very fast (~1 Hz) non-linear motions associated with internal "waves" in "solibore" form above sloping bottoms. Although such motions were captured with NIOZ1 (Hosegood et al., 2004), more detailed information was requested, even more than presented by Thorpe (1987) who used an array of 11 thermistors at, on average, 10 m spacing, sampling every 10 s to a resolution of 0.1 mK at ~3000 m depth off Porcupine Bank.

Except for Thorpe's measurements, also in shallow water (Thorpe and Hall, 1974), very few moored observations have been made of highly varying temperatures as a measure for density (ρ) variations. Such variations occur as internal waves supported by larger-scale stable density stratification, or as turbulence in mixing events. Both are

OSD

1, 37–64, 2004

related in a sense that internal waves can generate turbulence when they break. Temperature variations O(1 s) can be expected, as has been proven by observations using towed thermistor strings sampling the upper 100 m of the ocean at 0.1–4 Hz using 180 sensors at about 0.5 m intervals (Marmorino et al., 1987; Moum et al., 1992). However, as suggested from observations by Thorpe (1987) and Hosegood et al. (2004), such temperature variations can be expected even in deep-ocean environments, despite the local background buoyancy period, which is relatively large O(10–100 min). As a result, for monitoring such deep internal temperature variations standard thermistor strings sample too slow, and CTD and microstructure profilers suffer from the relatively slow lowering speed of typically $1\,m\,s^{-1}$.

The frequency (σ) of free propagating, linear internal gravity waves is limited to $f<\sigma<N$, $N \gg f$. At the low end, $f=2\Omega \sin\varphi$ denotes the local inertial frequency, the normal component of the earth's angular momentum vector $\mathbf{\Omega}$ measured at a latitude φ. At the high end, $N=\left(-g\frac{d\ln\rho}{dz}\right)^{1/2}$ the background buoyancy frequency, with g the acceleration of gravity, pointing in the downward, negative z-direction. The vertical length scale of N is crucial for the natural frequency of vertical oscillatory motion. As a result, N is one of the most important oceanographic parameters, and one of the most difficult to measure at the same time. Motions of all scales cause inherent density stratification changes (straining) of many different length and time scales (Pinkel et al., 1991), deforming the linear wave patterns. In the time domain, non-linear internal waves show steep ramps, i.e. sudden temperature changes within a period of less than 1 min only (Thorpe and Hall, 1974; Thorpe, 1987; Gemmrich and van Haren, 2001). Such steep waves may overturn when propagating in larger scale current shear (see many examples in Turner, 1973), thereby generating turbulent mixing. In the open ocean typical vertical mixing scales are several meters, unstability remaining for periods of several minutes–1 h, as determined using 3–4 min repeated CTD and microstructure profiles (Alford and Pinkel, 2000).

To study the individual overturning events, induced by internal waves above a deep sloping bottom, measurements are required of temperature variations in space and

time that go far beyond the buoyancy period and vertical length scale. The present specific aim is to have a thermistor string (NIOZ2) which resolves the finest non-linear internal wave fluctuations and scales of O(1 m) and O(1 s) and which is moored in combination with an acoustic Doppler current profiler (ADCP). The latter concurrently measures vertical profiles of all three current components.

2. Instrumentation

2.1. Technical aspects

Comparing NIOZ2 with NIOZ1 several technical differences are noted (Table 1). NIOZ1 uses 2 thermistors as part of a Wienbridge oscillator, the frequency of which can be very accurately measured. In contrast, NIOZ2 operates a single thermistor at 0.3 V DC in a Wheatstone bridge on a 24 bit A/D convertor. This results in much less precision (∼1 mK) compared to NIOZ1 (∼50 μK). However, the power consumption is greatly reduced. Also in NIOZ2 sampling is truly synoptic. The processing time of all 128 thermistors is only 0.2 s, so that sampling at 1 Hz is easily achieved inclusive data transport and storage, which is 20 times faster than NIOZ1.

In NIOZ2, the glass embedded thermistor plus electronics board are polyurethane encapsulated, held inside a titanium tube 13 mm in diameter and 120 mm in length. The titanium here serves the purpose of mechanical protection only. The advantage of titanium housing is less corrosion sensitiveness but the disadvantage is the greater difficulty in finding proper casting and primer materials to watertight the connections to the electric cables. Presently polyurethane resin is used (85 shore-A). To spread the risks of accidental leakage, the entire string is split up into 8 sections of 16 sensors. Each section separately powers 4 groups of 4 sensors. Depending on the type of failure, one either looses 1, 4 or 16 sensors at a time. This approach also allows for easy reconfiguration or replacement in the field. The drawback is the rather large amount of individual cables involved, which, for that reason, are kept as thin as pos-

sible. 16 cables from 16 sensors are led to 1 data concentrator, measuring 50 mm in diameter and 190 mm in length. 8 cables from 8 data concentrators are led to 1 central controller-datalogger-unit.

This central unit and the central battery unit are each held in a titanium container 150 mm in diameter and 520 mm in length. The data are logged in portions of 10.5 MB on a 512 Mb compact flash card using a Persistor CF-1 micro controller operating in PicoDos. The uploading of a full 512 Mb memory card takes only about 40 min (200 Kbaud) via an USB-port. As a fresh battery pack outlasts the filling of 512 Mb by a factor of 1.5–2 (depending on the sampling rate), the total period of measurements depends on the capacity of the memory card and on the sampling frequency, which can be chosen between 0.033 and 1 Hz. Although designed for short-term moorings sampling at high frequency, NIOZ2 can be moored for up to 400 days whilst sampling once every 30 s.

As the digital representations are non-linearly related to temperature, noise level is also a function of temperature, ranging from 0.4 mK at 0°C to 1 mK at 40°C. A "best achievable" laboratory calibration takes months and is a complicated activity, whilst the accuracy is not better than 3 mK (van Haren et al., 2001). As a result, like NIOZ1, NIOZ2 is calibrated in situ immediately before and after a deployment using a high-performance CTD: a much faster calibration. This calibration has a further advantage as it allows for a more precise calibration by limiting it to the expected temperature range measured locally, instead of performing a large range calibration. Also, because of the short duration of the calibration (several hours) depending on the depth levels, this calibration can be repeated more often to allow for the investigation of sensor drift. The calibration procedure is described in Sect. 3.2.

In NIOZ1 one could replace an individual sensor rather easily, but no cabling could be changed, as this consisted of a single umbilical. In NIOZ2, one may replace 1 segment, that is 16 sensors plus 1 concentrator, as the smallest interchangeable part. Presently, all electric cables, sensors and concentrators are taped to a 9 mm nylon coated steel cable. The 128 sensors are fixed at 0.5 m distances.

2.2. The mooring configuration

The central steel cable assures that the thermistor string can be moored in line. Generally, the thermistor string is moored in conjunction with an upward looking 300 kHz, 20° beam angle RDI-Sentinel ADCP mounted in a bottom landing frame. This mooring is recovered using two Benthos acoustic releases mounted in the frame, which uncouple simultaneously the thermistor string and the main 500 kg dropping weight from the bottom frame, so that the thermistor string and the bottom lander surface separately. Mooring motions are kept as low as possible by attaching the thermistor string under a single ellipsoidal buoy having 200 kg net buoyancy.

The thermistor string is attached to the centre of the bottom lander, with a 1 m horizontal off-set with respect to the central vertical axis of the ADCP. This ADCP does "hear" the thermistor string, but usually for brief periods of time only, and in a limited number of bins.

3. First results

During the first deployment of NIOZ2 at 3000 m depth at the foot of the continental slope in the Rockall Channel, a defect in the data storage software led to loss of all but calibration data. During the second deployment, reported here, problems were experienced with the encapsulation of the concentrators, so that 3 complete segments leaked and failed. Nevertheless, this second field experiment provided detailed temperature observations of internal waves and large non-linear bores.

The bottomlander mooring was located near the top of the eastern slope of Great Meteor Seamount (GMS), Canary Basin, North-Atlantic ocean (Fig. 1; Table 2). The mooring was deployed for ~5 days. The NIOZ2 recorder collected 185 MB of 1 Hz data from about 500 m depth. The mooring was not deployed deeper, because during the pre-deployment calibration the aforementioned casting material showed problems at pressures greater than about 200 Bars. Also, ADCP-data become poor when the

instrument is moored at angles of more than 15°. As GMS is very steep with typical slopes of 10–20° or more, a moderate slope was only found near the foot of the underwater mount at ∼4500 m depth and near its top between 450–550 m.

3.1. Environmental conditions

The upper ocean of the Canary Basin (CB, ∼30° N, 25° W, 5000 m water depth) shows a steppy rather than a smooth temperature decrease with depth (Fig. 2a), not just at the depth of ∼200 m where we find the main thermocline, but also at greater depths around 1500 m. Salinity also decreases with depth, except between 800 and 1200 m depth, as a result of Mediterranean outflow. As a result, double diffusive processes are expected to some extent around 1500 m explaining the steps. However, other small-scale variability in CTD-profiles also suggest important internal wave induced straining and occasional overturning. This holds for the waters above the abyssal CB plain, far away from boundaries, as well as for profiles obtained above rugged topography like GMS (Figs. 2a and 2b). It is noted that near-bottom overturning and stratification vary considerably with time. At times, stratification moves very close to the bottom, as can be seen in Fig. 2b (red curve) where it is only 1 m from the lowest point in the profile, or about 4 m from the bottom.

The detailed temperature profiles (Fig. 2b) from the depth range of the deployed NIOZ2, having sensors between 464 and 528 m depth, demonstrate a slight difference between GMS and the abyssal CB. Besides a change in temperature variation with depth due to current friction near the bottom of GMS, also a slight change is observed in large-scale temperature variation with depth up to 150 m above the bottom. This implies a change in the large-scale stratification. In the open ocean the 5 m N has a mean of ∼45 cpd over the depth range in Fig. 2b, although strongly varying between 0–80 cpd due to the small layers. As shown in Fig. 2c, the 5 m $N(450\,\mathrm{m}) \approx 60$ cpd observed above GMS, decreasing to ∼20 cpd around 500 m and increasing again to ∼45 cpd just above the bottom boundary layer, where it is negligibly small. This greater variability, also at large scales, near GMS, is likely related to typical sloping bottom

boundary layer processes and internal waves.

The CTD-profiles from different locations around the mooring site did not result in great differences in temperature-density relationship. Over the depth range between 420–580 m depth, slightly expanded with respect to the NIOZ2 depth range to cover the entire temperature range sampled by NIOZ2, $\delta\rho = -0.108 \pm 0.002 \delta T$ kg m^{-3} °C^{-1}, a reasonably tight relationship (Fig. 2d). As salinity decreased with depth it counteracted the temperature induced density gradient. Most of observed deviations from this linear relationship were due to mismatches of the CTD sensors that were difficult to mend even in post-processing. The environment was too variable, with density steps and mixed layers alternating quickly. Although mixed layers of several meters in the vertical were abundant, the variations with time caused some problems for the in-situ calibration of NIOZ2.

3.2. In-situ calibration

The thermistor string is coiled up on top of the Rosette-sampler protective cage surrounding a Seabird-911 plus CTD. The thermistor string's data-logger and battery units are located where one normally finds the water bottles. A protective netting is tied around the thermistor string. The distance between the CTD-temperature and pressure sensors and the thermistor string is about 1 m. After the thermistor string is started to sample at 1 Hz, the CTD is lowered following normal CTD-launch procedures. Online the downcast trace is inspected for steps of near-homogeneous waters of preferably a few m or more in vertical extent, in the temperature range anticipated during the deployment period. In practice this implies lowering the CTD to the depth of deployment; if the deployment site is on a sloping bottom the ship is moved a few km away from the slope. During the upcast the CTD is commanded to the selected depths of near-homogeneous water layer steps (Fig. 3a). The requirement is that the temperature varies less than 1 mK for a period of at least 90 s. To achieve this, CTD's temperature and pressure values are constantly monitored visually. Given the degree of non-linearity of the sensors 6–8 calibration values are sought for a temperature span

of 2–3°C. The electronic NIOZ2 data are translated to temperatures using a polynomial fit to the calibration values for each sensor separately. The above procedure takes about 3 h for calibration around 2000 m depth.

In general, the result of this in-situ calibration is not very much better than the laboratory calibration, due to the environmental variability, CTD frame vibrations and flow obstructions. Post-processing is required to achieve accuracy close to the 1 mK precision, which is shown for NIOZ2 in Fig. 4. Following the above procedure two more steps are required.

First, profiles of mean temperatures are computed over small periods of time ($\sim T_N$, the local large-scale buoyancy period) in which temperature is reasonably constant. These profiles are manually corrected to a new mean of a static stable temperature profile (Fig. 4a) under the assumption that overturns and small-scale instabilities are removed when averaged over such period. In practice, the corrections are constant shifts in temperature (Figs. 4b and 4d) and generally < 5 mK. They are attributed to impossibility of holding the calibration CTD long enough in constant temperature waters. This is concluded as this correction is valid for the entire period of observations each time the particular correction temperature is reached. As such, this first step is sufficient to have NIOZ2 observations accurate to within 1 mK over a short period of time (Figs. 4c and 4e). However, when this accuracy is required for the entire record, that is for the entire temperature range observed, another post-processing step is needed due to the non-linearity of the sensors.

Second, distributed over the entire temperature range of the record some 6-10 correction profiles as in Fig. 4 are constructed. Then, the calibrated data record is corrected by interpolation and replacing the means by the static stable means for each particular temperature in each sensor.

3.3. Temperature and current observations near the bottom of GMS

3.3.1. General temperature observations

An overview of the 5 days temperature record demonstrates the great variability of temperature in the bottom boundary layer above the 5° slope near the top of GMS (Fig. 5). The main variability has a semidiurnal tidal periodicity. A considerable discrepancy is observed between the temperature records from current meter sensors at 1.25 and 86 m ab ove the bottom (Fig. 5a). Away from the bottom the record shows many small-scale temperature fluctuations superimposed on the tidal signal. Very close to the bottom the record is much smoother than further up, but the non-linearity seems larger close to the bottom, forming a cnoidal shape of the tidal record, with occasional sharp ramps as near day 73.5. In detailed NIOZ2 observations like in Fig. 5b it appears that this ramp is extremely sharp, with a front passing the sensors with temperature dropping by 0.5°C within 1 s. Such fronts or bores were previously observed, at a rate of once/30 s, in continental slope regions like the Faeroe-Shetland Channel where they appeared at a 4 days periodicity (Hosegood et al., 2004) and the Bay of Biscay where tidal periodicity dominated (Gemmrich and van Haren, 2001). Apparently, such roaring, upslope motions resulting in strongly non-linear temperature profiles also exist at the sides of seamounts in the open ocean. The NIOZ2 details of this backwards breaking wave include overturning that resembles fingers as so accurately depicted by Hokusai-san for a surface wave with mount Fuji in the background.

Preceding and following such frontal passage, near-bottom temperature stratification varied considerably, although completely mixed bottom boundary layers of several tens of meters thick as in flat-bottom tidal seas were not observed. With the varying stratification many small-scale features were observed ranging from overturns (Sect. 3.3.3) to high-frequency internal waves (Sect. 3.3.4). The latter varied between 1 min periodicity waves, for example at day 73.62, and smooth 15 min waves, around day 73.7.

3.3.2. General ADCP observations

The ADCP measures all three components of current between 8–86 mab (445–523 m depth). The Cartesian (East, West, Vertical) current components are transferred to (offslope, alongslope, bottom normal) = (u, v, w) as in van Haren et al. (1994). Instead of the instrument tilt meter information, which gave a mean of 6.7° tilt, the bottom slope estimate of 4.5° from the ship's echo sounder is used. The ADCP's tilt meter is unreliable because the instrument is fixed, not gimballed in its frame. Also, local bottom relief may tilt the entire bottom-lander differently from the average slope angle. The ADCP also provides an "error velocity" e, which is the difference of currents between beam pairs and indicative of the current inhomogeneity across the beam spread (and/or a failure of one or more beams). As a result, its data can be used to qualitatively investigate quasi-turbulent overturning motions varying on scales <25 m horizontally and < several minutes in time. The system's output of e is modified by a factor of 4 cos(20°) to be comparable with the vertical currents (van Haren et al., 1994). Finally, the ADCP backscatter strength or echo intensity output I is used as a qualitative measure for variations in suspended material, turbulence and small-scale stratification. Instead of using the raw data that include the water attenuation of sound, the mean at each depth is subtracted; what remains is the relative echo intensity dI.

The amount of scatterers posed a problem on the data analysis: in general the s/n ratio was too low, presumably due to clear water (Fig. 6). As a result, it was impossible to perform a spectral analysis of these data, and direct estimations of vertical fluxes of heat and momentum were unreliable. Also, at some depths like at 19 mab the data were flawed by the zero-bias due to reflection off the thermistor string. Nevertheless, a general impression of the current variations with depth and time was obtained.

Like temperature, the bottom boundary currents and relative echo intensity are also dominated by semidiurnal tidal variations (Fig. 6). As is obvious from the currents, the observations start just after neaps and stopped just before springs. The cross-slope current generally has larger amplitudes than the along-slope tidal current. These tidal

currents are also not uniform in the vertical, with strongest currents usually, but not always, not too far off the bottom (∼10–20 mab). Additionally, strong high-frequency variability is observed, during which relatively large bottom-normal currents O(10^{-2} m s^{-1}) are observed. The lack of coherence between e and w, with e generally much smaller than w, implies confidence in measured w over scales larger than the beam width. Each tidal period has its own characteristics, with varying amplitudes and height of tidal and high-frequency motions and echo intensity.

An example of a single tidal period (Fig. 7) shows the common features, of which the details may vary, 1. asymmetry in $u-$ (and $v-$, not shown) currents with height, with near bottom currents always leading those higher up, 2. a sudden transition to upslope motion as in Hosegood et al. (2004), 3. many high-frequency waves in both u and w, but not in e. Such waves exist up to 80 mab and have periods of typically 15 min $\approx 2T_N$, T_N the large-scale buoyancy period, as observed previously in the North Sea (van Haren et al., 2001), 4. these high-frequency motions are internal waves as evident from the high-resolution temperature measurements (especially from the panel with $\partial T/\partial z$, which demonstrate that the "homogeneous" bottom boundary layer may extend up to 40 mab during the up-slope phase of the tide, but also that stratification is capping a very thin bottom boundary layer of less than 5 m during the down-slope phase. Especially during this phase (between days 73.3–73.4) e is non-negligible, evidence of current inhomogeneity across the beam spread, or small-scale motions, during which most overturns are observed in the NIOZ2 data (unstable temperature gradients). The turbulence generated during the down-slope phase is expected from classic Ekman theory, but the detailed observation of a thin pycnocline close to the bottom is unexpected.

3.3.3. Temperature overturns

NIOZ2 revealed the character of some of the occasional small-scale temperature instabilities (Fig. 8). Such instabilities appeared in a more or less regular sinusoidal waveform in a temperature time series (Fig. 8b), but they were related to a backwards

breaking wave or rolling-up of a Kelvin-Helmholtz instability (Fig. 8c). Although such overturning waves have been observed in the ocean at shallow depths using photography (Woods, 1968) and temperature profiling (Thorpe and Hall, 1974), the present observations are the first detailed observations at great depth. The large-scale overturn of more than 10 m in height, and the associated very thin layers of enhanced stratification of ∼1 m, take about 1 min to pass the sensors. As they are only poorly resolved by the ADCP sampling "only" once per 30 s, such NIOZ2 observations emphasize the need to sample fast to capture processes relevant for many large scale motions, as is expected from boundary mixing on the interior large-scale flow. Such fast sampling is not only required for large-scale "turbulent" motions, but also for small-scale waves, as is demonstrated below.

3.3.4. (Too) short internal waves

NIOZ2 also revealed occasional "regular" small-scale temperature variations (Fig. 9) that appeared to have periods of several minutes, much less than the local buoyancy period of 20–30 min (Fig. 2c), no matter how small the vertical length scale was chosen to compute stratification. The detailed plot (Fig. 9) shows both the instrumental capability in the occasionally very smooth temperature records hiding the 1 mK noise and the occasionally quite noisy environmental background, with noise levels of O(10 mK), especially also during the passage of a wave (e.g. between days 73.6185–73.62). These particular waves, which have a period of 3 min, are tilted at an angle to the vertical. If such waves existed as free propagating internal waves their upward "phase" propagation would imply downward energy propagation. However, their observed frequency $\sigma_o \gg N$, computed over 5 m vertical intervals. Computing the intrinsic frequency $\sigma = N = \sigma_o - U \cdot k$, $U \approx 0.3\,\mathrm{m\,s^{-1}}$, we require $k \approx \sigma_o / U \approx 1/150$ cpm for free internal waves, so that the wavelength $\lambda \approx 20$ m. Apparently the short waves are generated and Doppler shifted by the larger scale internal waves. They appear as interfacial waves, generating turbulence, as they "move" at the fringe of breaking.

This can also be seen in a second example of even smaller scale waves, having

periods less than 1 min, "carried" below the crest of an ∼18 min N-wave (Fig. 10). The NIOZ2 is capable of resolving both the 30 s "wave", as well as coherent and incoherent motions within that small wave, which both exist as cool water intrusions under the N-wave.

4. Summary

We have presented some data from a newly built fast responding thermistor string, which is capable of measuring temperature variations in the deep ocean at an estimated precision better than 1.5 mK, sampling 128 sensors synchronously at a rate of 1 Hz for a period of up to 15 days at depths down to 6000 m. In this configuration each single vertical temperature profile of 64 m is sampled about 50–100 times faster than using a standard CTD. During the construction and first trials the sensors turned out very robust, but a major problem was found in the proper bonding of polyurethane casting resin to titanium.

The response and sampling time in combination with its endurance have shed new light for studies on internal waves near sloping bottoms up to the highest frequencies, including non-linearities like internal bores. The latter appear irregularly at a relatively large time scale of several hours – days, but pass the sensors within a few minutes. As the importance of internal wave induced mixing is more and more recognized, also in conjunction with the large-scale ocean circulation, such detailed studies are needed to learn more about such mixing processes. Previously, these detailed studies have been performed in laboratory experiments (e.g. McEwan, 1983) or near the surface of the ocean (e.g. Woods, 1968; Marmorino et al., 1987; Moum et al., 1992), but very limited in the deep ocean (Thorpe, 1987). Especially the transfer of energy from the large scale to the small mixing scales is a field that hitherto was impossible to explore with deep-ocean observations. In the examples given in this paper clearly the Doppler-shift of small internal waves to the point of breaking is observed, as well as shear-induced Kelvin-Helmholtz instabilities. The appearance of bores or thermal

fronts during the upslope phase of the tide remains a subject of study, especially also because we have not yet established the underlying reason why the magnitude of a bore varies so strongly between the different (tidal) periods.

Acknowledgements. We thank the crew of the R. V. Pelagia for deploying the "mixBB" bottom lander. We thank participants of the yellow tape-team, who taped NIOZ2 several times to its strength member: T. Hillebrand, K. Veth and P. Hosegood. M. Hiehle composed Fig. 1. The development of the NIOZ fast thermistor strings and the deployment in the Canary Basin were financed by investment grants ("Oceanographic equipment" and "LOCO", respectively) from the Netherlands organisation for the advancement of scientific research, NWO.

References

Alford, M. H. and Pinkel, R.: Observations of overturning in the thermocline: the context of ocean mixing, J. Phys. Oceanogr., 30, 805–832, 2000.

Gemmrich, J. R. and van Haren, H.: Thermal fronts generated by internal waves propagating obliquely along the continental slope, J. Phys. Oceanogr., 31, 649–655, 2001.

Hosegood, P., Bonnin, J., and van Haren, H.: Solibore-induced sediment resuspension in the Faeroe-Shetland Channel, Geophys. Res. Lett., 31, L09301, doi:10.1029/ 2004GL019544, 2004.

McEwan, A. D.: The kinematics of stratified mixing through internal wavebreaking, J. Fluid Mech., 128, 47–57, 1983.

Marmorino, G. O., Rosenblum, L. J., and Trump, C. L.: Fine-scale temperature variability: the influence of near-inertial waves. J. Geophys. Res., 92, 13 049–13 062, 1987.

Moum, J. N., Hebert, D., Paulson, C. A., and Caldwell, D. R.: Turbulence and internal waves at the equator. Part I: statistics from towed thermistors and a microstructure profiler, J. Phys. Oceanogr., 22, 1330–1345, 1992.

Pinkel, R., Sherman, J., Smith, J., and Anderson, S.: Strain: observations of the vertical gradient of isopycnal vertical displacement, J. Phys. Oceanogr., 21, 527–540, 1991.

Thorpe, S. A.: Current and temperature variability on the continental slope, Phil. Trans. R. Soc. Lond., A 323, 471–517, 1987.

Thorpe, S. A. and Hall, A. J.: Evidence of Kelvin-Helmholtz billows in Loch Ness, Limnol. Oceanogr., 19, 973–976, 1974.
Turner, J. S.: Buoyancy Effects in Fluids. Cambridge University Press, Cambridge, 1973.
van Haren, H., Garrett, C., and Oakey, N.: Measurements of internal wave band eddy fluxes above a sloping bottom, J. Mar. Res., 52, 909–946, 1994.
van Haren, H., Groenewegen, R,. Laan, M., and B. Koster, B.: A fast and accurate thermistor string, J. Atmos. Oceanic Technol., 18, 256–265, 2001.
Woods, J. D.: Wave-induced shear instability in the summer thermocline, J. Fluid Mech, 32, 791–800, 1968.

Table 1. Specifications of NIOZ fast thermistor strings. Compared to the very precise NIOZ1 the new NIOZ2 is somewhat less precise but much faster, sampling many more sensors.

	NIOZ v.1	***NIOZ v.2***
Number of sensors	32 (at 1 m intervals)*	128 (at 0.5 m intervals)*
Thermistors	2 per sensor	1 per sensor
Depth rating	6000 m	6000 m
Range (T)	-5 .. 55 °C	-2 .. 50 °C
Accuracy	better than 0.5 mK	1.5 mK
Noise level	≅ 20 μK	≅ 1 mK***
Self heating	≅ 300 μK	≅ 1000 μK
Response time (τ)	< 0.25 s (in water)	< 0.25 s (in water)
Total sampling time	<4 s (for 32 sensors)	0.5 s (for 128 sensors)
Minimal sampling interval (Δt)	20 s	1 s
Memory and battery life	100 days (Δt = 30 s; 32 sensors)	15 days (Δt = 1 s;128 sensors)+

* Maximum distance between sensors. Lines are flexible to make sensor distances smaller.

** Siemens Matsushita B57017-K822.

*** Noise level is temperature dependent. Worst case is denoted here.

+ 512 MB Flash card installed. Sufficient power capacity to upgrade to 2 GB.

Table 2. Instrument details of ADCP-NIOZ2 mooring between 11 March 2003 and 16 March 2003 at 29°59.876′ N, 28°18.906′ W, 531 m depth, bottom slope ~0.079 (4.5°). (*ls* = lowest sensor; *fb* = first bin).

Instrument	Depth (m)	Sampl. int. (s)
Nortek AquaDopp	445	30
Aanderaa RCM11	446	60
NIOZ2	528.15 (*ls*)	1
RDI 300 kHz ADCP	529.75 (*fb*: 523.2)	30

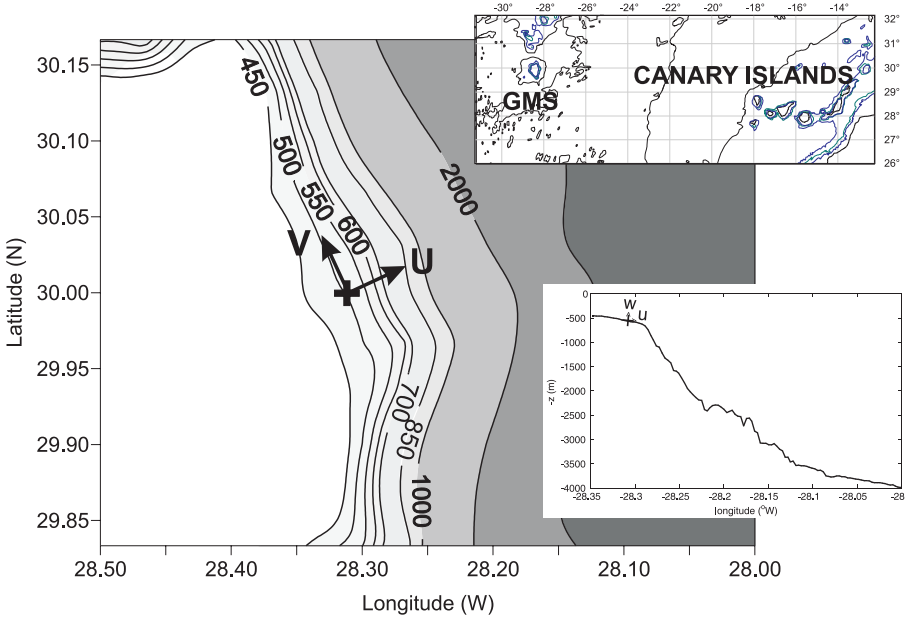

Fig. 1. Mooring site and Cartesian coordinate current components near the top of Great Meteor Seamount (GMS) at the western edge of the Canary Basin.

OSD

1, 37–64, 2004

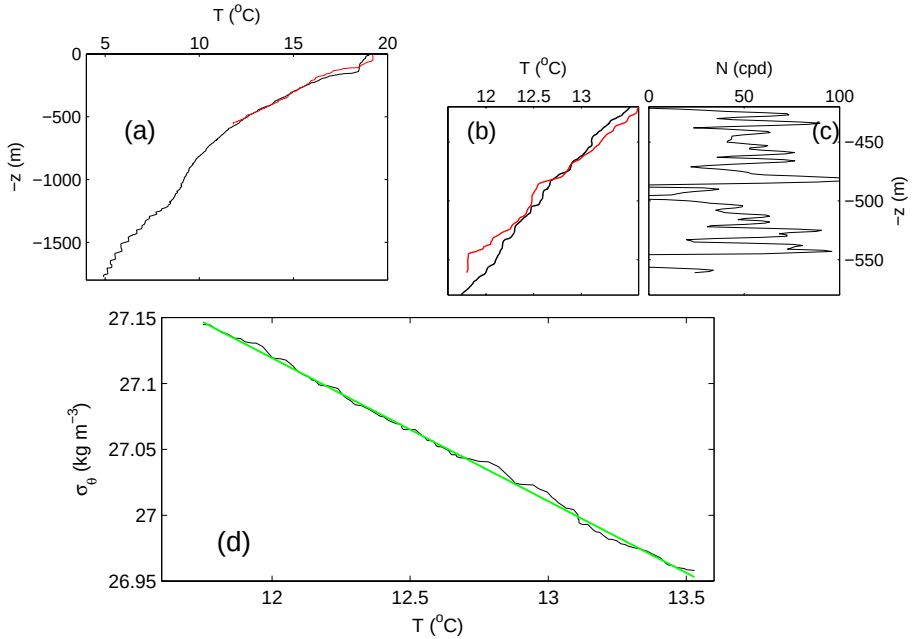

Fig. 2. Environmental conditions from 24 Hz CTD observations in the Canary Basin around the depth of the NIOZ2 mooring site at GMS. **(a)** Temperature, 2 m vertically smoothed profiles from CTD01: 31.75° N, 21.41° W, 4957 m depth (black) and from CTD02: 30.01° N, 28.32° W, 563 m depth (red). **(b)** Detail of (a), with the black graph for raw 24 Hz CTD01-data. **(c)** N computed over 5 m intervals for CTD02. **(d)** Temperature-density anomaly plot, depth interval as in (b) and (c), for CTD01 with the corresponding linear relationship in green.

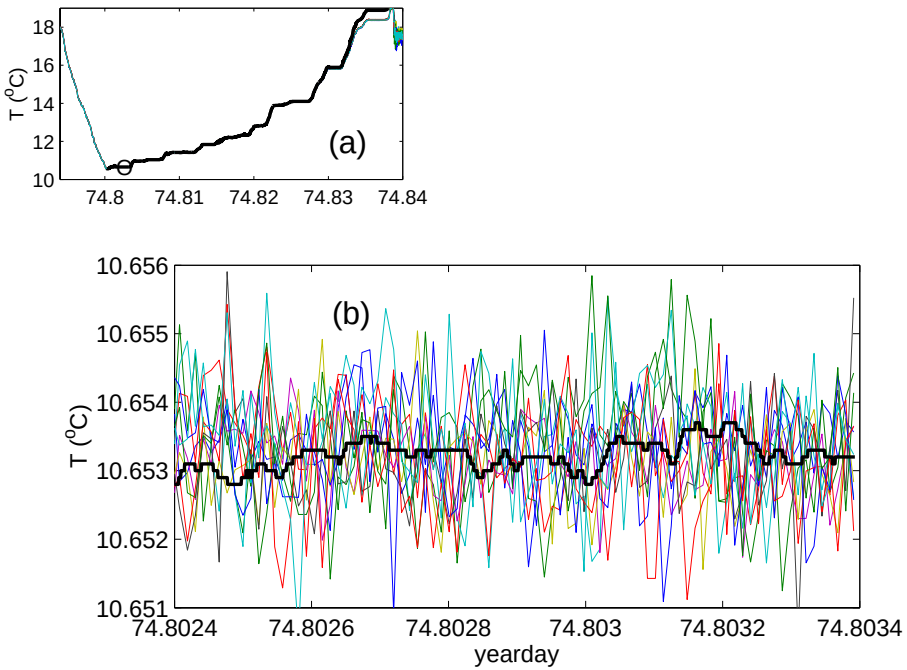

Fig. 3. In situ calibration of NIOZ2 using CTD. **(a)** Calibrated NIOZ2 temperatures from 10 sensors (colours), and upcast trace of CTD (black) demonstrating the 7 steps between 11–14°C when the CTD is held in a layer of "constant" temperature. Non-linearity is visible as the CTD and NIOZ2 traces do not match anymore in the upper right corner. **(b)** Noise or precision comparison in 86 s of the record in (a) (in circle), demonstrating the higher noise rate of the thermistors (std: 0.7 mK as opposed to 0.2 mK for the CTD), also showing some of the environmental variability in the ~20 s waves appearing in CTD data.

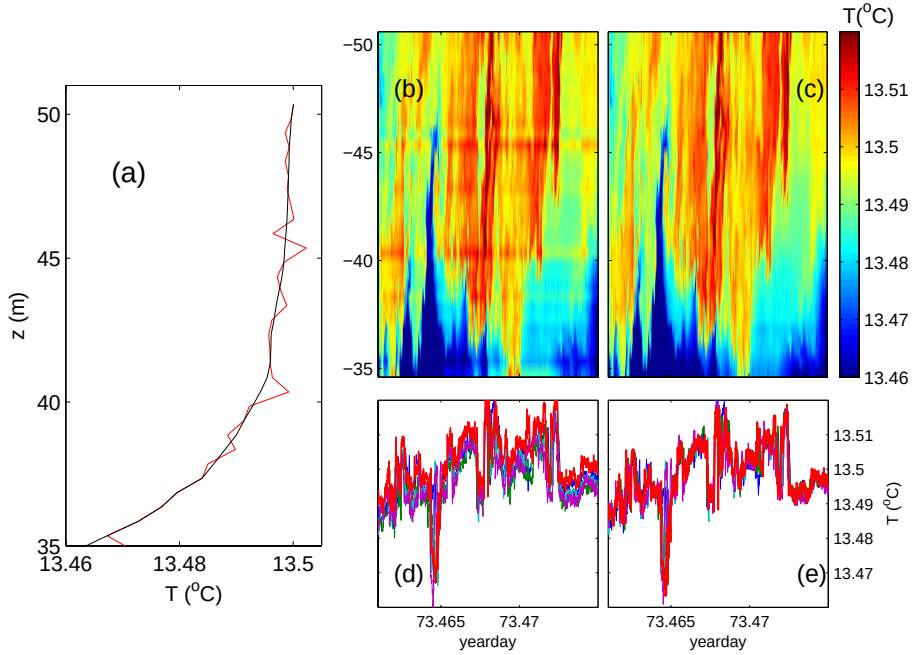

Fig. 4. Example of post-processing following in situ calibration of NIOZ2. **(a)** Mean profile for 32 sensors of the data portion in (b): uncorrected in red and corrected in black. **(b)** Uncorrected 22 mins of data for 32 sensors halfway up NIOZ2 moored at GMS. **(c)** As (b), but corrected following (a). **(d)** Four temperature traces from (b). observed between 45–47 m above the bottom (mab). **(e)** As (d), but corrected, demonstrating the trace at 46 mab no longer displaced with respect to the others.

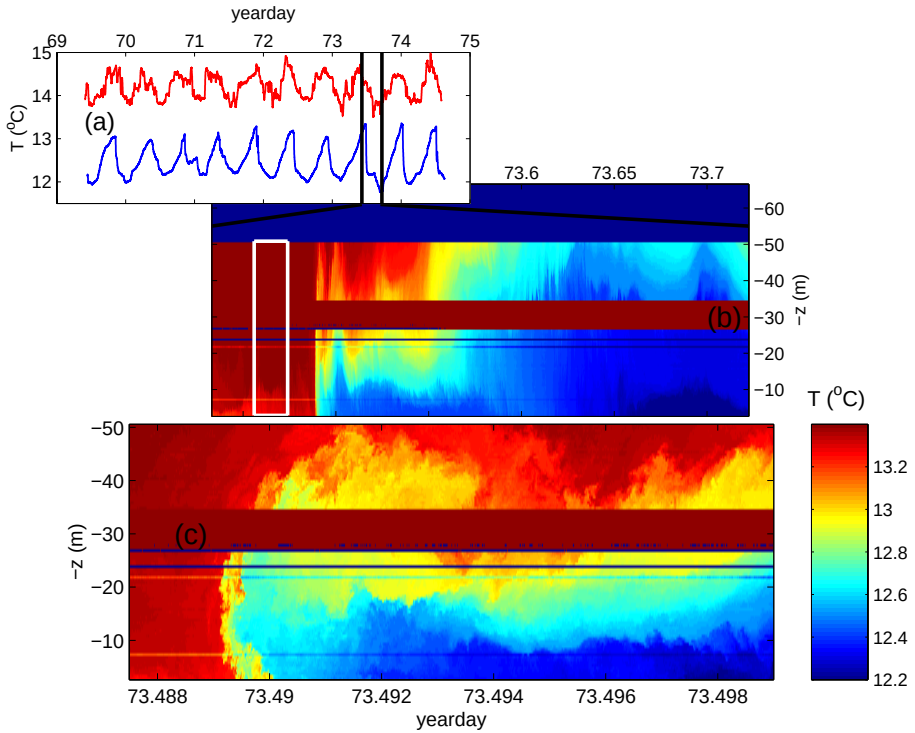

Fig. 5. **(a)** Time series of temperature during the entire mooring period at GMS measured by the ADCP at 1.25 mab and by a current meter moored above NIOZ2 at 86 mab (Table 2). **(b)** Detail of 10 h of NIOZ2 temperature demonstrating a sharp near-bottom front. The blue bar above 52 mab indicates two failing segments, the brown bar around 30 mab one failing segment; otherwise 3 sensors were bad as well. The white rectangle is studied in more detail in Fig 8c. Further detail of 17 min of NIOZ2 data around the passage of the front.

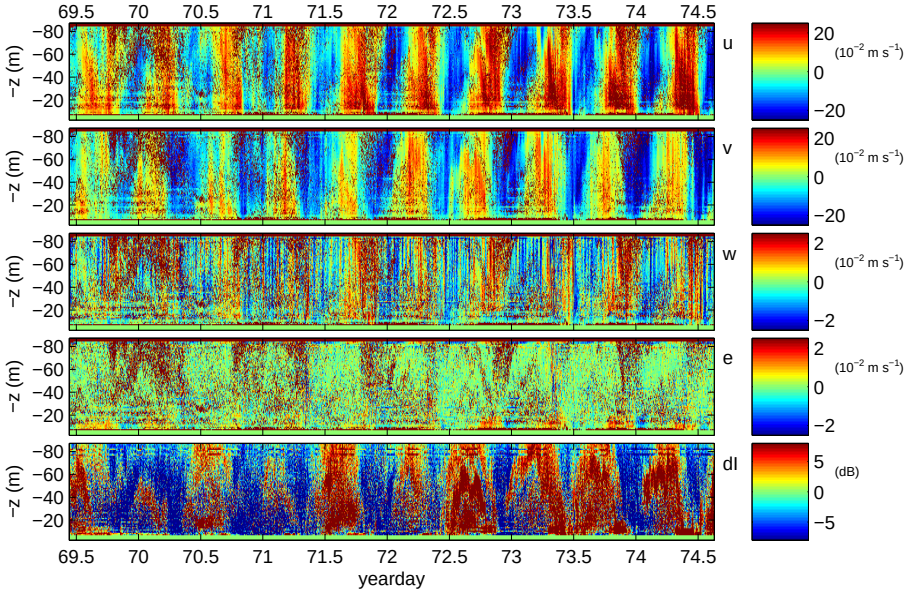

Fig. 6. Overview of ADCP observations between 7.8 and 86.8 mab. In addition to the three current components cross-slope (u), along-slope (v) and bottom-normal (w) the corrected "error" velocity (e) and the relative backscatter strength (dI) are shown. The brown speckles throughout the graphs indicate "bad data", of which there are many, implying that the amount of scattering material was low, and varying with time and depth.

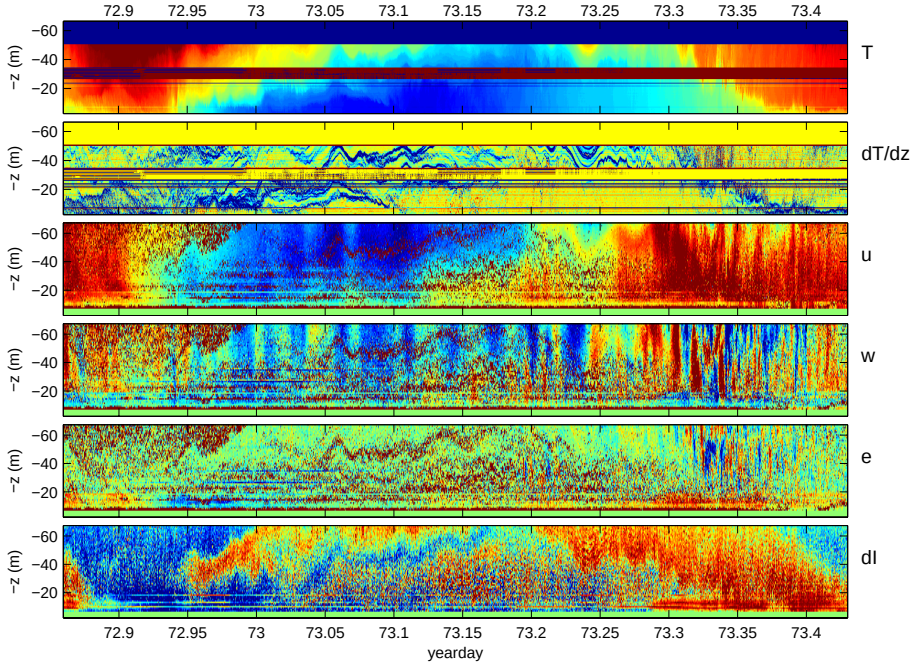

Fig. 7. A typical tidal period of NIOZ2 and ADCP observations between 2.8 and 66.8 mab. In addition to temperature (T) also its vertical derivative (dT/dz $\sim N^2$) is shown in the second panel. From the ADCP data the cross-slope (u), bottom-normal (w) and the corrected "error" velocities (e) are shown above the relative backscatter strength (dI) are shown. The colouring from blue-red is similar to Fig. 6 for the ADCP data; for T it is between [11.8, 13.4]°C. For $\partial T/\partial z$ the colours are between [−0.04, 0.025]°C m^{-1} with blue-green indicating stable stratification, yellow indicating neutral and orange-red indicating unstable overturning.

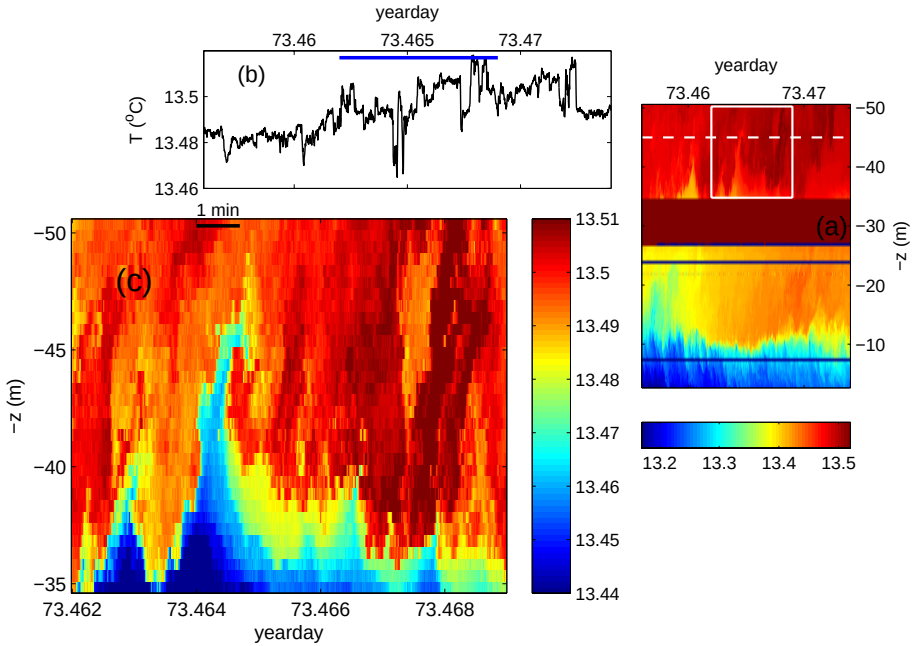

Fig. 8. Example of detailed observation of an overturn, ∼12 m breaking wave around 40 mab. **(a)** Corrected data from the rectangle in Fig. 5b showing temperature stratification and very high-frequency (∼1 min) temperature variations down to the sensors closest to the bottom. The temperature at the depth of the white dashed line is plotted in **(b)**. Demonstration of irregular short-term temperature variations, including a cross-section through an overturn around day 73.464 and a temperature anomaly at day 73.468. The blue bar denotes the period of **(c)**. Detail from the white rectangle in (a) showing a large overturning wave of Kelvin-Helmholtz instability (Turner, 1973).

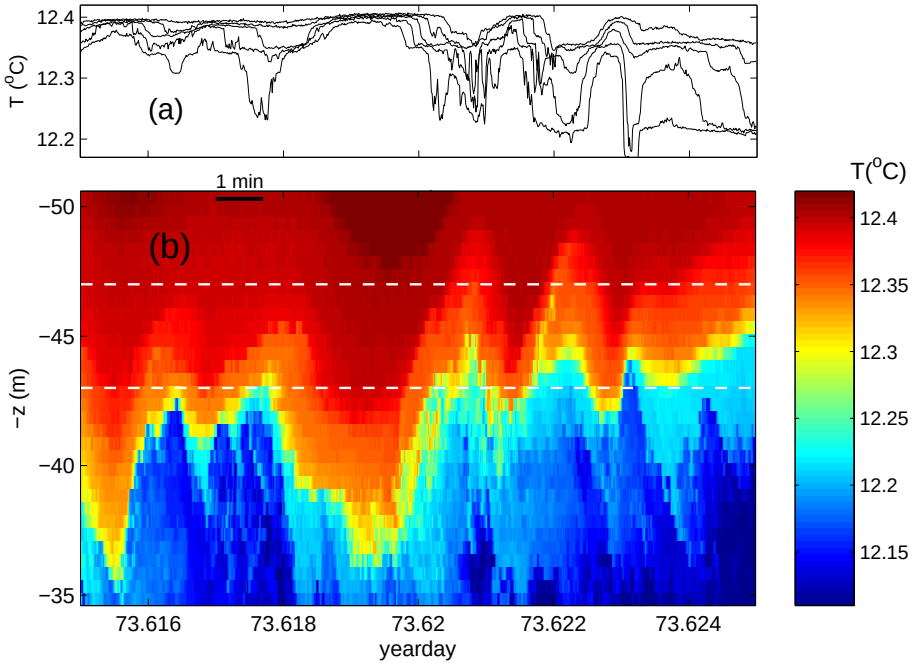

Fig. 9. Example of detailed NIOZ2 observation of very high-frequency internal "wave". **(a)** Temperature contours from 5 sensors at 1 m intervals between the white dashed lines in **(b)**. Contour plot using information of all sensors, separated by 0.5 m, in the depth-time interval shown.

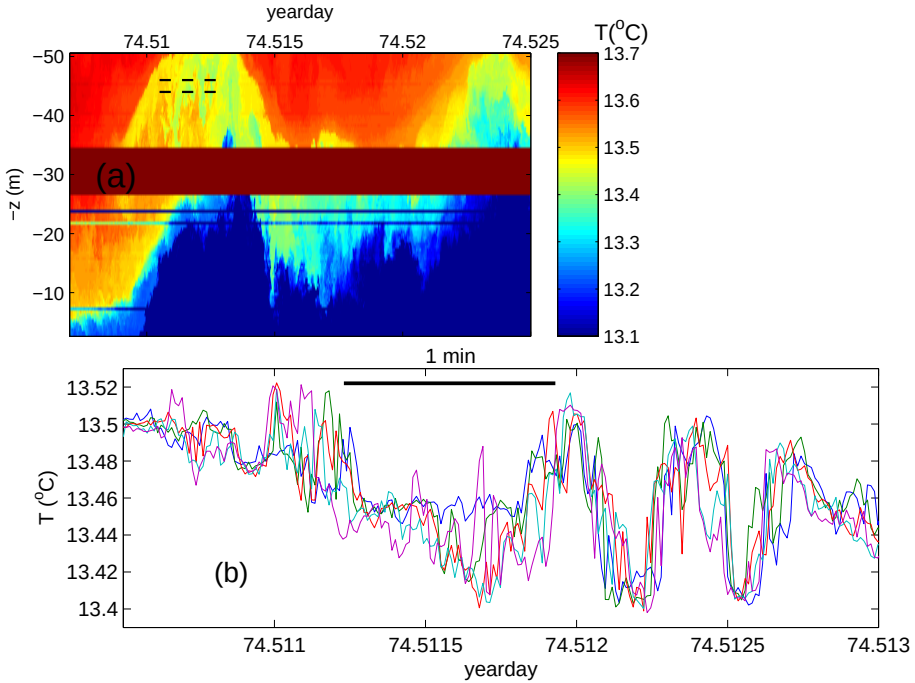

Fig. 10. Example of detailed NIOZ2 observation of very high-frequency internal "wave" of unstable fluid. **(a)** Contour plot showing lower temperature water (green; between days 74.51–74.514; $38<z<50$) in an environment of warmer water under the crest of a large-scale wave having a period near the local buoyancy period. The dashed black lines in the small-scale "wave" indicate the depth levels and time range of the temperature series in **(b)**.